Int J Adv Manuf Technol (2010) 51:587–598
DOI 10.1007/s00170-010-2629-z

ORIGINAL ARTICLE

Modeling and analysis of the edge disintegration in the EDM drilling cobalt-bonded tungsten carbide

Nun-Ming Liu · Ko-Ta Chiang · Jenn-Tsong Horng · Chih-Cherng Chen

Received: 21 January 2010 / Accepted: 15 March 2010 / Published online: 12 April 2010

Abstract The characteristic feature of edge disintegration easily appears in the electric discharge machining (EDM) drilling processing of cobalt-bonded tungsten carbide (WC-Co). Such tendency reduces the strength against fatigue and results in a poor assembly tolerance. The objective of this paper was to present the mathematical models for modeling and analysis of the effects of process parameters, including the discharge current, pulse time on, duty factor, and capacitance value, on the disintegration factor at the entrance edge of drilled hole in the EDM drilling process of cobalt-bonded tungsten carbide. An experimental plan of a central composite design based on the response surface methodology (RSM) was employed to carry out the experimental study. The quadratic model of RSM associated with the sequential approximation optimization method was used to find the optimum settings of processing parameters. With the experimental values up to a 95% confidence interval, it is fairly well for the experimental results to present the mathematical model of disintegration factor. The results show that the interaction effect of discharge current with capacitance value has the greatest influence on the disintegration factor, followed by the capacitance value and the quadratic term of duty factor. The optimal settings of processing parameters obtained in this study represent the reduction of the 5.53% disintegration factor, which were compared with the results of initial processing parameters for drilling the cobalt-bonded tungsten carbide in the EDM process.

Keywords Disintegration · Drilling · Cobalt-bonded tungsten carbide · Response surface methodology · Electric discharge machining (EDM)

N.-M. Liu (✉) · K.-T. Chiang · J.-T. Horng
Department of Mechanical Engineering,
Hsiuping Institute of Technology,
No. 11, Gungye Rd.,
Dali City, Taichung, Taiwan 41280, Republic of China
e-mail: nunming58@yahoo.com.tw
e-mail: nunming58@gmail.com

K.-T. Chiang
e-mail: kota@mail.hit.edu.tw

J.-T. Horng
e-mail: vgear2001@yahoo.com.tw

C.-C. Chen
Department of Automatic and Control Engineering,
ChungChou Institute of Technology,
No. 6, Lane 2, Sec. 3, Shanjiao Rd., Yuanlin Town,
Changhua, Taiwan 51001, Republic of China
e-mail: jcchen@dragon.ccut.edu.tw

1 Introduction

The cobalt-bonded tungsten carbide (WC-Co), a kind of engineering conductive ceramic components, possesses exceptional mechanical properties such as high strength, high hardness, and high toughness [1, 2]. Although the major portion of machining applications of this type of cemented tungsten carbide is used as cutting tools, the scope of alternative applications is quickly growing such as molding material of metal forming, forging, squeeze casting, and high-pressure die casting. The typical processes of cobalt-bonded tungsten carbide are compacting techniques of powder metallurgy and high-temperature sintering. However, it is very difficult and expensive for such materials to produce complex shapes with high-dimensional accuracy through conventional machining techniques. To machine hard and brittle ceramic materials by traditional cutting machinery can cause the cracks on the machined surface [3]. Electric discharge machining (EDM) is the best choice for

machining the conductive ceramic materials because there is no contact between the tool and workpiece during all over the EDM process. In the EDM process, the surface layer of the workpiece can be rapidly melted and removed by an arc of 8,000–12,000°C at each charging point. EDM takes advantage of the spark erosion principle to machine the hard-to-cut material and then to produce the required shapes and sizes, finer surface properties, and better dimensional accuracy. Over the past few years, EDM has been widely applied in the modern metal industry for producing intricate and complex shapes required for conductive ceramic materials that are difficult to manufacture by conventional machining [4, 5].

Drilling macro- or microholes with a high aspect ratio is one of the most important, frequently practiced, and unavoidable machining operations. The EDM drilling process overcomes the defects of the convectional twist drilling process, such as high tool wear, tool breakage and burr formation, etc. Jeswani [6] first investigated small drilling holes in the high carbon steel using the EDM process with copper wire electrode. Jain [7] analyzed the effect of pulse time, bit type of tool, and depth of penetration on the performance characteristic of EDM drilling in the high-speed steel. Uno et al. [8] demonstrated that the fine boring of drill high aspect ratio holes in monocrystalline silicon ingot were achieved by the electrical discharge machining process with high efficiency. Wang and Yan [9] made use of the rotary EDM concept to drill the blind holes in the Al_2O_3/6061Al composite. Asokan et al. [10] investigated the effect of EDM parameters on the deep-hole drilling of titanium alloy using copper electrode. Mohan et al. [11] researched the machinability of Al–SiC metal matrix composite by drilling holes using the rotary hollow tube electrodes in the EDM process. Kumagai et al. [12] developed a new composite electrode, a metal rod enclosed in a dielectric fluid pipe, to prevent secondary side sparks in the EDM so as to drill narrow deep holes in the steel block. Pham et al. [13] studied the influence of various factors contributing to microelectrode wear during EDM drilling with microrod and microtube electrodes. Kuppan et al. [14] made an experimental investigation of small deep-hole drilling of Inconel 718 in the EDM process to understand the effect of process parameters on the machining characteristics.

However, the application of EDM drilling process to machine the hard and brittle ceramic materials can easily cause cracks on the machined surface for lack of some suitable processing parameters. With regard to the surface cracks of drilled hole, the characteristic feature of edge disintegration easily appears in the drilling of the hard and brittle ceramic materials. Disintegration is caused by the electrical spark discharge in which high-temperature and strong discharge impact results in rapid evaporation and melting in the edge of hole. Such tendency occurrence would reduce the strength against fatigue and result in a poor assembly tolerance. The main objective of this paper was to present the mathematical models for modeling and analysis of the effects of processing parameters on the disintegration factor at the entrance edge of drilled hole in the EDM drilling process of cobalt-bonded tungsten carbide. The mathematical models are developed using response surface methodology (RSM) to explain the influences of process parameters, including the discharge current, pulse time on, duty factor, and capacitance value, on the disintegration characteristics in the EDM drilling process. The RSM is an empirical modeling approach for determining the relationship between various process parameters and responses with the various desired criteria and searching for the significance of these process parameters on the coupled responses. It is a sequential experimentation strategy for building and optimizing the empirical model. Therefore, RSM is a collection of mathematical and statistical procedures that are useful for the modeling and analysis of problems in which response of demand is affected by several variables and the objective is to optimize this response [15–17]. By using experiments and applying regression analysis, the modeling of the desired response to several independent input variables can be obtained. Consequentially, the RSM is utilized to accurately describe and identify the influence of the interactions of different independent variables on the response when they are varied simultaneously. In addition, it is one of the most widely used methods to solve the optimization problem in the manufacturing environments [18–22]. Furthermore, the present study applies the quadratic model of RSM associated with a sequential approximation optimization (SAO) method to find the optimum settings of processing parameters on the disintegration characteristics in the EDM drilling process.

2 Experimental details

2.1 Equipment used in the experiments

The experiments were conducted using a CNC super drilling EDM machine, model DNC-35 manufactured by Aristech Industries, Taiwan. The electrode fixed to a special rotary head provides rotary motion in the process of feeding downwards into workpiece. The electrode rotating device includes a precision spindle, a rotary head drive mechanism, and a speed control unit. The spindle was designed with built-in seals to effect flushing through the electrode.

The copper tubular wire electrode (inner diameter, 0.10 mm; outer diameter, 0.20 mm) was used as tool, deionized water was used as the dielectric liquid, and the flushing injection of dielectric fluid was adopted to assure the

Table 1 EDM operating conditions

Working conditions	Unit	Description
Workpiece		94WC-6Co (100×100×10 mm^3)
Electrode material		Copper
Electrode polarity		Negative
Electrode rotation	rpm	300
Diameter of drilling hole	mm	0.20
Depth of drilling hole	mm	10
Open discharge voltage	V	110
Discharge current (I_P)	A	1–5
Pulse on time (τ_P)	μs	2–25
Duty factor (D_F)		0.25–0.85
Capacitance value (C_V)	μf	0.2–1.0
Dielectric fluid		Deionized water
Flushed pressure	gf/cm^2	2.5

adequate capability to flush the debris from the gap zone during the EDM process. The physical properties of copper electrodes are a melting point of 1,360 K, density of 8.94 g/cm^3, thermal conductivity of 226 W/mK, and electrical resistivity of 17.1 nΩm. The jet flushing system was employed to provide an impinging jet through the front end of the tubular electrode. The dielectric fluid was flushed at a pressure of 245 kPa through the tubular wire electrode. Table 1 shows the setting of experimental parameters under drilling the cobalt-bonded tungsten carbide in the EDM.

2.2 Material used in the experiments

The workpiece material used in this study is cobalt-bonded tungsten carbide (94WC-6Co, Protool Industrial Co.) which is composed of approximately 94% of tungsten carbide (WC) and 6% of cobalt (Co). This material was frequently used for the cutting tools due to its excellent hardness properties (HRA 92.8). Although the major portion of machining applications of this type of cemented tungsten carbide is used as a cutting tool, the scope of alternative applications is quickly growing, such as molding material of metal forming, forging, squeeze casting, and high-pressure die casting. Furthermore, it possesses a high compressive strength (5.7 GPa) as well as a good resistance to wear and oxidation at high-temperature status. The compound materials of tungsten carbide were mixed with Co in a certain proportion in order to provide high resistance to thermal shock. It has a density of 14.9 g/cm^3, a thermal conductivity of 100 W/mK, and a thermal expansion coefficient of 4.3×10^{-6} K^{-1} at a temperature of 200°C.

2.3 Experimental procedure

The experimental specimens of cobalt-bonded tungsten carbide used in the experiment were cut to be a rectangular block of 100×100×10 mm^3. Before experimentation, the top and bottom faces of workpiece were ground by a surface grinding machine, and the front end of tubular wire electrode was polished with a fine-grade emery sheet simultaneously. According to the bibliography in the EDM field and the results of related experiments, the electrode used in this study was subjected to a negative polarity in order to ensure the promotion of good surface quality [1–3]. The completion and position of small hole were machined and controlled using CNC software.

2.4 Design of the experiments

2.4.1 Machining performance evaluations

The disintegration around the holes was measured using the central composite design (CCD) color photograph of toolmakers microscope to pick the point data, following the schema presented in the Fig. 1. Measuring the maximum diameter (D_{max}) in the damage zone around each drilled hole presents the value of disintegration factor

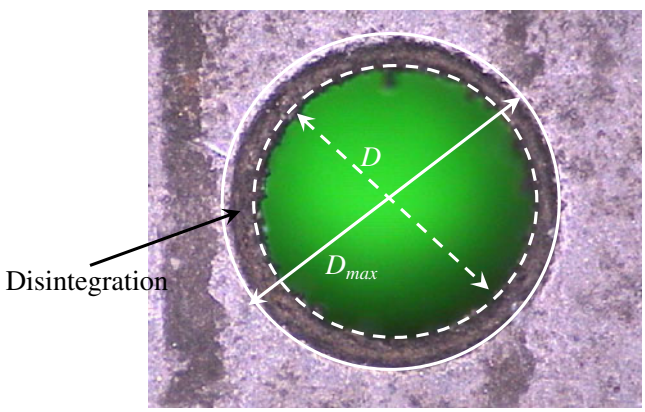

Fig. 1 Disintegration around the hole

(F_D). This factor is determined by the ratio the maximum diameter (D_{max}) of damage zone to the diameter (D) of hole, defined in the following

$$F_D = \frac{D_{max}}{D}. \quad (1)$$

2.4.2 Experimental design

In the experimental design, the experimental plans were designed on the basis of the CCD technique. The factorial portion of CCD is a full factorial design with all combinations of the factors at two levels (high, +1, and low, −1) and composed of the eight star points and the six central points (coded level 0) which are the midpoints between the high and low levels. The star points are at the face of the cube portion on the design that corresponds to an $\alpha = \pm 2$, and this type of design is commonly called the "face-centered CCD."

The controllable variables chosen for the experimentation were discharge current (I_P), pulse time on (τ_P), duty factor (D_F), and capacitance value (C_V). Here, the duty factor is defined as follows:

$$\text{Duty factor } (D_F) = \frac{\text{pulse time on}}{\text{pulse time on} + \text{pulse time off}}. \quad (2)$$

In addition, the discharge circuit of this CNC super drilling EDM machine used in the experiments was designed as the resistance–capacitance circuit (RC circuit) which provides higher peak current, lower pulse time on, and discharging sparks at the bottom of the electrode. Therefore, this type of circuit greatly suits the small-area machining and the small-hole drilling. The control of capacitance values was recognized as one of the most important processing factors using this equipment. Other processing factors such as open discharge voltage, dielectric flushing pressure, and machining servo sensitivity were kept constant during the experimentation. At this moment, the electrode used in this study was subjected to a negative polarity owing to the promotion of good surface quality. Table 2 shows the controllable parameters and their levels in the coded and actual values.

In this study, the experimental plan was conducted using the stipulated conditions according to the face-centered CCD, and it involved a total of 30 experimental observations at four independent input variables. Each combination of experiments was carried out two times at different times under the same conditions to acquire a more accurate result. The experimental matrix adopted in this study in the coded form is shown in Table 3. The coded values $X_{i,i\ =\ 1,2,3,4}$ of the processing parameter used in Tables 2 and 3 were obtained from the following transformable equations:

$$X_1 = \frac{I_P - I_{P0}}{\Delta I_P} \quad (3)$$

$$X_2 = \frac{\tau_P - \tau_{P0}}{\Delta \tau_P} \quad (4)$$

$$X_3 = \frac{D_F - D_{F0}}{\Delta D_F} \quad (5)$$

$$X_4 = \frac{C_V - C_{V0}}{\Delta C_V} \quad (6)$$

where X_1, X_2, X_3, and X_4 are the coded values of parameters I_P, τ_P, D_F, and C_V, respectively. I_{P0}, τ_{P0}, D_{F0}, and C_{V0} are the values of I_P, τ_P, D_F, and C_V at zero level. ΔI_P, $\Delta \tau_P$, ΔD_F, and ΔC_V are the intervals of variation in I_P, τ_P, D_F, and C_V, respectively.

3 Mathematical modeling

The RSM is an empirical modeling approach for determining the relationship between various processing parameters and responses with the various desired criteria and searches for the significance of these process parameters in the coupled responses [15–17]. It is a sequential experimentation strategy for building and optimizing the empirical model. Therefore, RSM is a collection of mathematical and statistical procedures and is good for the modeling and analysis of problems

Table 2 Design schema of processing parameters and their levels

Parameters	Unit	Levels				
		−2	−1	0	+1	+2
Discharge current (I_P), X_1	A	1	2	3	4	5
Pulse time on (τ_P), X_2	μs	5	10	15	20	25
Duty factor (D_F), X_3		0.25	0.40	0.55	0.70	0.85
Capacitance value (C_V), X_4	μf	0.2	0.4	0,6	0.8	1.0

Table 3 Design layout and experimental results

Run	Coded factors				Actual factors				Response variable
	X_1	X_2	X_3	X_4	I_P	τ_P	D_F	C_V	Disintegration factor (F_D)
1	0	0	+2	0	3	15	0.85	0.6	1.097
2	0	0	0	0	3	15	0.55	0.6	1.065
3	0	0	0	0	3	15	0.55	0.6	1.065
4	0	0	0	+2	3	15	0.55	1	1.047
5	+2	0	0	0	5	15	0.55	0.6	1.114
6	+1	−1	+1	−1	4	10	0.7	0.4	1.077
7	0	−2	0	0	3	5	0.55	0.6	1.082
8	−1	+1	+1	−1	2	20	0.7	0.4	1.069
9	+1	+1	+1	−1	4	20	0.7	0.4	1.129
10	0	0	0	0	3	15	0.55	0.6	1.065
11	−2	0	0	0	1	15	0.55	0.6	1.084
12	−1	+1	−1	+1	2	20	0.4	0.8	1.079
13	+1	+1	−1	+1	4	20	0.4	0.8	1.095
14	0	0	−2	0	3	15	0.25	0.6	1.110
15	0	0	0	0	3	15	0.55	0.6	1.065
16	−1	−1	+1	+1	2	10	0.7	0.8	1.084
17	+1	−1	+1	+1	4	10	0.7	0.8	1.036
18	−1	−1	−1	+1	2	10	0.4	0.8	1.127
19	−1	−1	−1	−1	2	10	0.4	0.4	1.089
20	0	0	0	0	3	15	0.55	0.6	1.065
21	+1	+1	+1	+1	4	20	0.7	0.8	1.043
22	+1	−1	−1	−1	4	10	0.4	0.4	1.133
23	0	0	0	0	3	15	0.55	0.6	1.063
24	+1	+1	−1	−1	4	20	0.4	0.4	1.133
25	0	+2	0	0	3	25	0.55	0.6	1.103
26	+1	−1	−1	+1	4	10	0.4	0.8	1.099
27	−1	+1	−1	−1	2	20	0.4	0.4	1.100
28	−1	−1	+1	−1	2	10	0.7	0.4	1.101
29	−1	+1	+1	+1	2	20	0.7	0.8	1.102
30	0	0	0	−2	3	15	0.55	0.2	1.098

in which the desired response is affected by several variables. The mathematical model of the desired response to several independent input variables is gained using the experimental design and applying regression analysis.

In this study, the quantitative form of relationship between desired response and independent input variables can be represented in the following:

$$Y = f(I_P, \tau_P, D_F, C_V) \tag{7}$$

where Y is the desired response and f is the response function (or response surface). In the procedure of analysis, the approximation of Y was proposed using the fitted second-order polynomial regression model which is called the quadratic model. The quadratic model was exactly suitable for studying carefully the interactive effects of combinative factors on the performance evaluations. The quadratic model of Y can be written as follows:

$$Y = a_0 + \sum_{i=1}^{4} a_i X_i + \sum_{i=1}^{4} a_{ii} X_i^2 + \sum_{i<j}^{4} a_{ij} X_i X_j \tag{8}$$

where a_0 is constant and a_i, a_{ii}, and a_{ij} represent the coefficients of linear, quadratic, and cross product terms, respectively. X_i reveals the coded variables corresponding to the studied machining parameters. Here, the value of the disintegration factor (F_D) indicated as Y was analyzed. The model using the quadratic model of f in this study aims not only to investigate the response over the entire factor space but also to locate the region of desired target where the response approaches its optimum or near optimal value.

In general, the quadratic model of desired response (Y) can be expressed in the matrix form as follows:

$$Y = \mathbf{X}\alpha + \varepsilon \tag{9}$$

where $\mathbf{X}$ is a matrix of model terms evaluated at the data points and ε is an error vector. The unbiased estimator ε of the regression coefficient vector a is estimated using the least-squares error method as follows.

$$\alpha = \left(\mathbf{X}^{\mathrm{T}}\mathbf{X}\right)^{-1}\mathbf{X}^{\mathrm{T}}Y \tag{10}$$

where $\mathbf{X}^{\mathrm{T}}$ is the transpose of the matrix $\mathbf{X}$.

Consequently, the RSM is a sequential procedure, and its procedure for modeling and analysis of the effects of process parameters on the edge disintegration in the EDM drilling cobalt-bonded tungsten carbide steel, including six steps, is summarized in the following:

1. Defining the independent input variables and desired responses with the design constraints;
2. Adopting the face-centered CCD to plan the experimental design;
3. Performing the regression analysis with the quadratic model of RSM;
4. Calculating the statistical analysis of variance (ANOVA) for the independent input variables and hunting which parameter significantly affects the desired response;
5. Determining the situation of the quadratic model of RSM and deciding whether the model of RSM needs screening variables or not;
6. Conducting confirmation experiment and verifying the predicted performance characteristics.

4 Results and discussion

4.1 Deformation of disintegration in the edge of drilled hole

At the beginning stage of EDM drilling process, the electrical spark discharge solely impacts the machined surface of cobalt-bonded tungsten carbide steel in which high-temperature and strong discharge impact result in rapid evaporation and melting in the entrance edge of hole. The impact effect of electrical spark discharge becomes more noticeable as the value of discharge current rises due to the higher spark energy which produces more and larger disintegrations on the machined surface of the hole's entrance. Figure 2 depicts the status of disintegrations under the discharge current (I_{P}) 2A and 4A, respectively, while the other processing factors were kept constant. These figures obviously reveal the status of disintegration under the high value of discharge current. Therefore, the conditions of discharge energy at the discharge point relates to the status of disintegration in the edge of the drilled hole. The discharge energy also determines the rate of melting and evaporation at the discharge point which affects the form and depth of drilled hole. In this study, the experimental specimens adopted the cobalt-bonded tungsten carbide which has high hardness property (HRA 92.8). The EDM drilling process of cobalt-bonded tungsten carbide must possess discharge energy which is large enough to pass through and form the drilled hole. But the larger discharge energy easily presents the status of disintegration for the hard and brittle ceramic material.

4.2 Analysis of the proposed quadratic mathematical model

In order to ensure the goodness of fit of the quadratic model obtained in this study, the test for significance of the regression model, the test for significance on individual model coefficients, and the test for lack-of-fit need to be performed [15–17] as shown in Table 4. These tests are performed as ANOVA procedure by calculating the "F value," the "Prob. > F", the determination coefficients (R^2), adjusted R^2 (R^2 Adjusted), and the adequate precision (AP). The values of "F value" and the "Prob. > F" imply statistical significance on the regression model and the particular linear, quadratic, or interaction terms. Usually, as the desired confidence level is set to 95%, a value of "Prob. > F" smaller than 0.05 signifies that the regression model is considered to be statistically significant, which is desirable as it demonstrates that the terms in the model have a significant effect on the responses. The determination coefficient R^2 is defined as the ratio of the explained variation to the total variation and is a measure of the degree of fit. When R^2 approaches unity, the better the response model fits the actual data, the less the difference between the predicted and actual values exists. The adjusted R^2 (R^2 Adjusted) presents a measure of the amount of variation around the mean explained by the model, adjusted for the number of terms in the model. R^2 Adjusted decreases as the number of terms in the model increases if those additional terms do not add value to the model. Furthermore, the value of AP in this model, which compares the range of the predicted value at the design point to the average prediction error, is well above 4. The value of the ratio is >4, which presents the adequate model discrimination. These models obtained higher values of the R^2, R^2 Adjusted, and AP at the same time. In Table 4, the model fitting assessment for the quadratic model of disintegration factor (F_{D}) is based on the statistical parameters above.

From the results of Table 4, the values obtained were as follows: R^2=0.9895, R^2 Adjusted=0.9394, and AP= 10.2786 for the disintegration factor (F_{D}). Consequently, the obtained quadratic mathematical models for the disin-

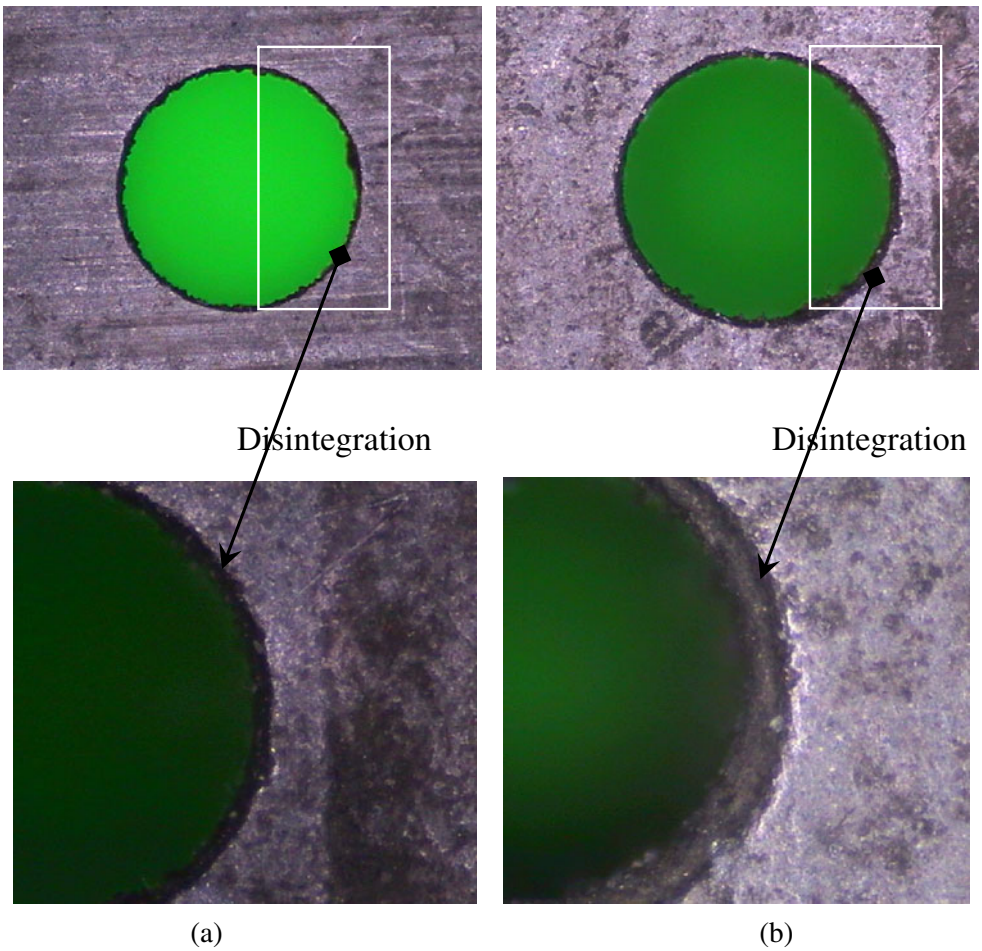

Fig. 2 Disintegration around the hole under the discharge current (I_P) 2 A (**a**) and 4 A (**b**)

tegration factor (F_D) can be regarded as significant effect for fitting and predicting the experimental results, and meantime, the test of lack-of-fit also displays to be insignificant.

Table 5 shows that the values of "F value"' and "Prob. > F" for each term on the performances of the disintegration factor (F_D). The $X_1(I_P)$, $X_2(\tau_P)$, $X_3(D_F)$, $X_4(C_V)$, X_1^2, X_2^2, X_3^2, X_1X_3, and X_1X_4 can be regarded as significant terms because their "Prob. > F" values are <0.05. The backward elimination process eliminates the insignificant terms to adjust the fitted quadratic models. These insignificant model terms can be removed, and the test of lack-of-fit

Table 4 ANOVA for the fitted models

Final quadratic models	Disintegration factor (F_D)
f value	5.5995
Prob. > F	<0.0001
R^2	0.9895
R^2 Adjusted	0.9394
Adequate precision (AP)	10.2786
Lack of fit	Not significant

Table 5 Results of the ANOVA

Symbol	Degree of freedom	Disintegration factor (F_D)	
		F value	Prob. > F
$X_1(I_P)$	1	7.8631	0.0438[a]
$X_2(\tau_P)$	1	8.3837	0.0467[a]
$X_3(D_F)$	1	11.5045	0.0040[a]
$X_4(C_V)$	1	14.1731	0.0019[a]
X_1^2	1	9.9144	0.0066[a]
X_2^2	1	6.7468	0.0202[a]
X_3^2	1	12.5847	0.0029[a]
X_4^2	1	0.5915	0.4538
X_1X_2	1	3.3509	0.0871
X_1X_3	1	5.6370	0.0314[a]
X_1X_4	1	15.7197	0.0012[a]
X_2X_3	1	2.1356	0.1645
X_2X_4	1	0.9826	0.3373
X_3X_4	1	0.9240	0.3517
Residual	15		
Total	29		

[a] Indicates the significant term

also displays to be insignificant. Through the backward elimination process, the final quadratic models of response equation in terms of coded factors are presented as follows:

$$Y = 1.0673 + 0.0022\,X_1 + 0.0019\,X_2 - 0.0101\,X_3 - 0.0112\,X_4 + 0.0084\,{X_1}^2 + 0.0069\,{X_2}^2 + 0.0096\,{X_3}^2 - 0.0086\,X_1X_3 - 0.0143\,X_1X_4 \quad (11)$$

In terms of actual factors the final quadratic models of response equation are as follows:

$$F_D = 1.1669 + 0.0264\,I_P - 0.0079\,\tau_P - 0.3604\,D_F + 0.1600\,C_V + 0.0084\,{I_P}^2 + 0.0003\,{\tau_P}^2 + 0.4234\,{D_F}^2 - 0.0574\,I_P\,D_F - 0.0719\,I_P\,C_V \quad (12)$$

The above mathematical model can be used for predicting the values of F_D within the limits of the factors studied. The differences between the measured and predicted response are illustrated in Fig. 3. From the results of comparison, it proved that the predicted values of F_D are close to those readings recorded experimentally with a 95% confidence interval. Figure 4 displays the normal probability plot of the residuals for the disintegration factor (F_D). Notice that the residuals generally fall on a straight line, which implies that the errors are normally distributed. Furthermore, it adequately supports the least-squares fit.

4.3 The effect of processing parameters on the disintegration

The influences of processing parameters on the performance of the disintegration factor (F_D) have been analyzed based on the above proposed mathematical model in Section 4.2. According to the results in ANOVA, a sensitivity analysis for the processing parameters on the values of the disintegration factor (F_D) performed is shown in Fig. 5. From the results of percent contribution for each processing parameter, the first three significant factors on the value of the disintegration factor (F_D) are the I_PC_V, C_V, and ${D_F}^2$ with contributions of 14.94%, 13.47%, and 11.96%, respectively. It demonstrates that these three process parameters play major roles for the value of disintegration in the edge of drilled hole.

As for the EDM process, the electrical spark erosion process occurred successively, and then the removal of melt brings about the form of crater on the machined surface. The amount of melt removal determines the degree of material removal rate (MRR). Therefore, the degree of MRR also affects the form rate of machined hole in the EDM drilling process. The general trend of increase in the MRR with increase in the discharge current is clearly observed. The increase of the discharge current causes an increase in the discharge energy at the discharge point to improve the rate of melting and evaporation. But the more and larger disintegrations presented in the entrance edge of the drilled hole increase with an increase in the higher spark energy. Figure 6 shows the response surface and contour plot for the disintegration factor (F_D) in relation to the discharge current (I_P) and pulse time on (τ_P), with the duty factor and capacitance value maintained at the middle levels. In general, both the discharge current and the pulse time on determine the status of input energy in the EDM process. From Fig. 6, it can be seen that an increase in both the high value of discharge current and pulse time on leads to an increase of the disintegration factor (F_D). As the pulse time on ranges between 5 and 10 μs, the value of F_D first decreases with an increase of discharge current before 3 A

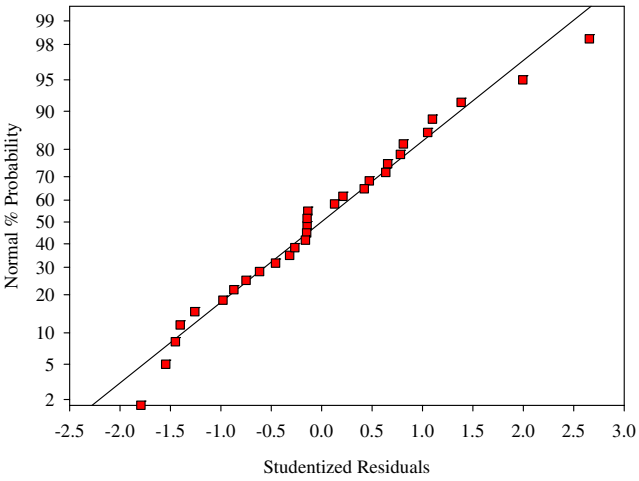

Fig. 4 Normal probability plot of the residuals for the disintegration factor (F_D)

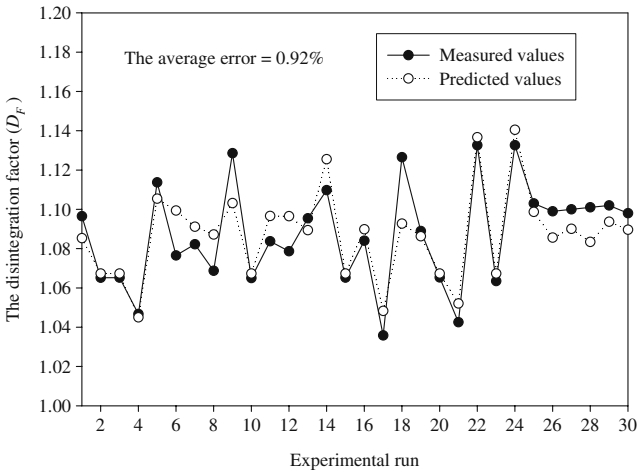

Fig. 3 Comparison of the measured and predicted values of the disintegration factor (F_D)

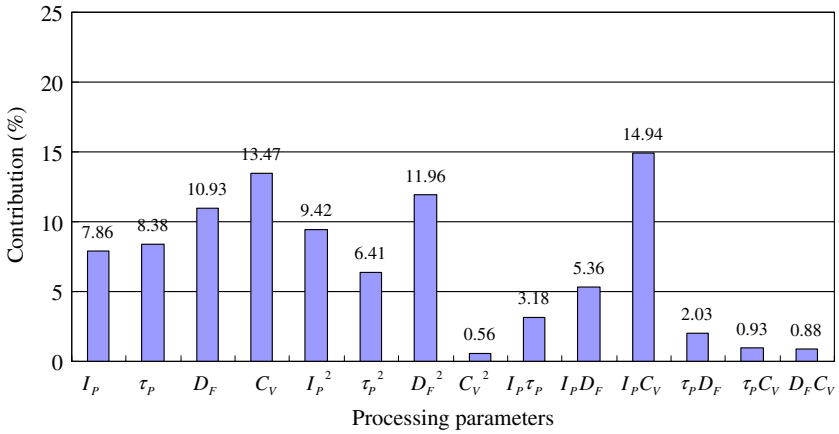

Fig. 5 Sensitivity analysis of processing parameters on the disintegration factor (F_D)

and then increases with a further increase in the discharge current. Similarly, the F_D value first decreases with an increase of pulse time on before 15 μs and then increases with a further increase in the pulse time on within the lower value of the discharge current (1–3 A). This result has been attributed to the lower discharge energy which does not produce more and larger disintegrations in the entrance edge of the drilled hole.

Figure 7 depicts the influences of discharge current (I_P) and duty factor (D_F) on the disintegration factor (F_D) with keeping the other two processing parameters at the middle levels. The increase of the duty factor means applying the spark discharging time for a long time, and this will cause an increase in the discharge times and machining efficiency and subsequently an increase in the amount of melted material removal. It is clear that the values of F_D increase with an increase of duty factor within the lower value of the discharge current (1–3 A). But the value of F_D decreases with an increase of both the high value of discharge current and duty factor. When both the discharge current and duty factor are set on the high level, the discharge energy density is enlarged on the electrical discharge spot, and it possesses larger discharge energy to pass through rapidly and to form the drilled hole. The retention period of spark discharging time in the entrance of machined surface is short, which results less and small disintegrations in the entrance edge of drilled hole.

In the electrical circuit of EDM, the capacitance component possesses the stable action of electrical spark erosion process. When the electrical discharge process presents the status of stability, the melt and the evaporation stably occur at the discharge point. Therefore, the entrance edge of the drilled hole reveals less and small disintegrations, which presents the good quality of the drilled hole.

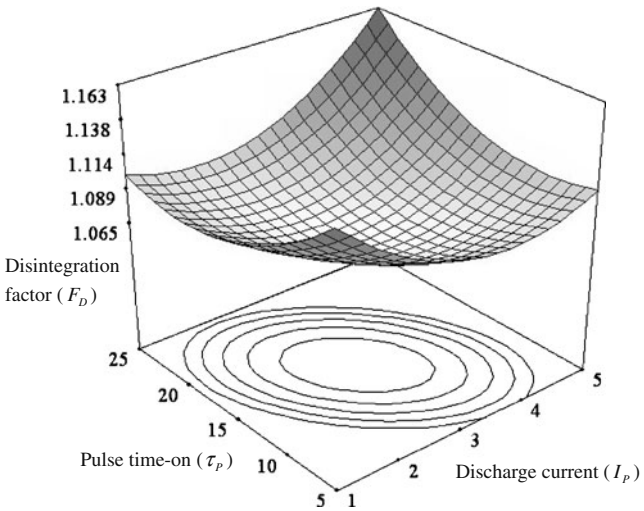

Fig. 6 Response surface and contour plot of disintegration factor (F_D) between the effect of discharge current (I_P) and pulse time on (τ_P) at D_F=0.55 and C_V=0.6

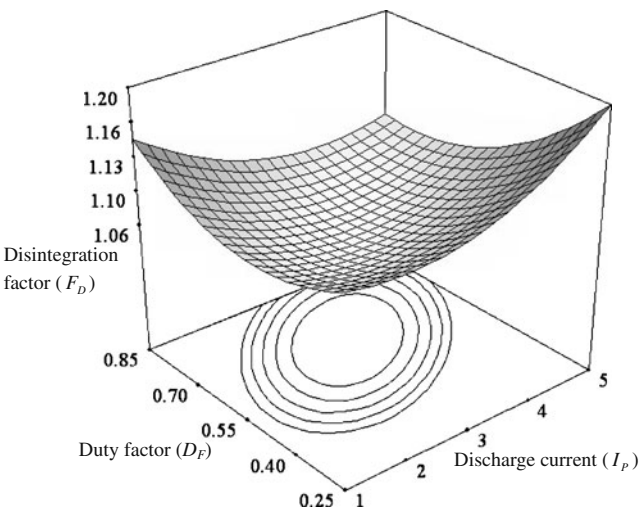

Fig. 7 Response surface and contour plot of disintegration factor (F_D) between the effect of discharge current (I_P) and duty factor (D_F) at τ_P= 15 μs and C_V=0.6

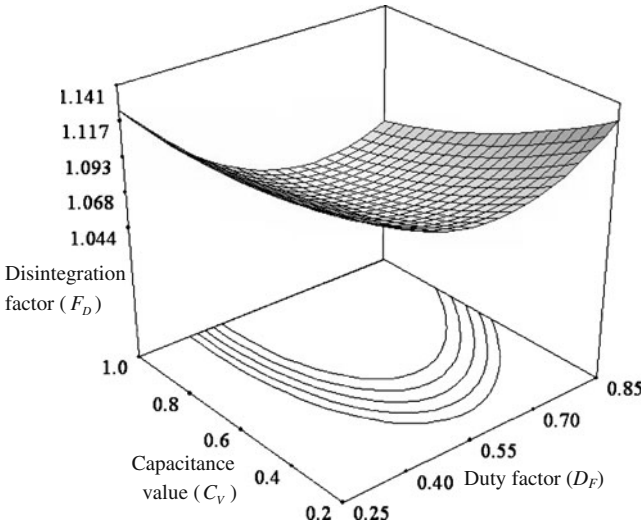

Fig. 8 Response surface and contour plot of disintegration factor (F_D) between the effect of duty factor (D_F) and capacitance value (C_V) at I_P=3 A and τ_P=15 μs

Figure 8 depicts the effect of duty factor (D_F) and capacitance value (C_V) on the disintegration factor (F_D) under the discharge current of 3 A and pulse time on of 15 μs. In Fig. 8, the value of F_D is shown to increase with an increase of the capacitance value. It is obviously shown within the higher value of duty factor.

The effects of discharge current (I_P) and capacitance value (C_V) on the value of the disintegration factor (F_D) under the pulse time on of 15 μs and duty factor of 0.55 are presented in Fig. 9, which shows that the value of F_D generally increases with an increase of the capacitance value within the lower discharging current. But it also reveals that the value of F_D apparently decreases with an increase of the capacitance value within the higher discharging current. This result has been attributed to the capacitance component, which also possesses the functions of delay and improvement in the discharge of electrical current. With the status of lower discharging current, the capacitance component improves the discharge energy at the discharge point which presents the possibility of more and larger disintegrations in the entrance edge of the drilled hole. When the discharging current is set on a higher level, the capacitance component delays the impact of discharge energy which benefits the quality of entrance edge of the drilled hole. As discussed above, because of the increase of discharge energy density, the effect of discharge current affects the disintegration factor as shown in Fig. 9.

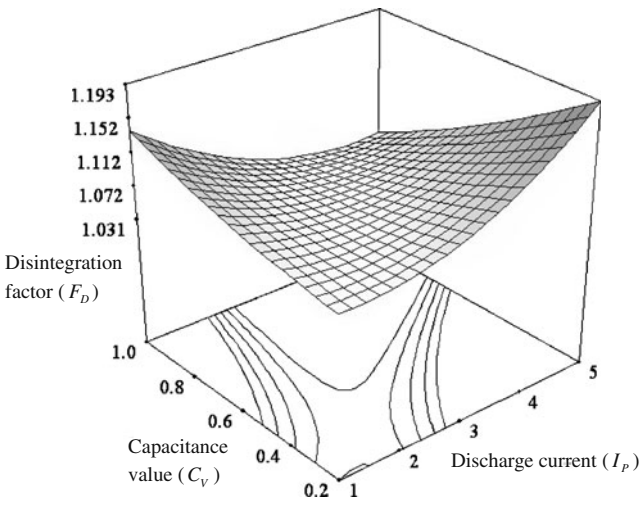

Fig. 9 Response surface and contour plot of disintegration factor (F_D) between the effect of discharge current (I_P) and capacitance value (C_V) at τ_P=15 μs and D_F=0.55

4.4 Optimization of processing parameters

In this study, the goal of optimization for the processing parameters in the EDM drilling process is to find the optimal values of processing parameters (X) in order to achieve the high quality of drilled hole. The optimal objective includes the target of desired dimensions on the minimum of disintegration factor (F_D). This optimization problem can be approximated by the following equations and then solved by means of the SAO method. The method makes use of an objective function, $f(X)$, called the desirability function. It reflects the desirable ranges for each response. For simultaneous optimization, each response must have a low and high value assigned to each goal. The SAO strategy in the RSM applies the approximate procedure, which is iteratively repeated until convergence.

$$\text{Find } X = [I_P, \tau_P, D_F, C_V] \tag{13}$$

$$\text{to minimize } f(X) = F_D \tag{14}$$

$$\text{subject to } 1 \le I_P \le 5 \text{ A}, 5 \le \tau_P \le 25\ \mu\text{s} \tag{15a}$$

$$0.25 \le D_F \le 0.85,\ \ 0.2 \le C_V \le 1.0\ \ \mu\text{f}. \tag{15b}$$

Table 6 Results of verification experiment and optimization condition

Case	Processing parameters				Spring-back angle ($\Delta\theta$)		
	I_P	τ_P	D_F	C_V	Exp.	Pred.	Error (%)
1	1	5	0.25	0.2	1.104	1.109	−0.45
2[a]	3	15	0.55	0.65	1.065	1.067	−0.19
3[b]	4.95	16.68	0.84	0.91	1.008	1.006	0.20
4	5	25	0.85	1.0	1.052	1.047	0.48

[a] The initial condition

[b] The optimal condition

Table 6 presents the results obtained from the four processing parameters with the optimum adjusts found by the SAO method in the RSM. The optimum processing parameters obtained in Table 6 are found to be discharge current (I_P) of 4.95 A, pulse time on (τ_P) of 16.68 μs, duty factor (D_F) of 0.84, and capacitance value (C_V) of 0.91 μf. The overall desirability is about 0.998 in accordance with the optimal conditions. As shown in Table 6, the performance evaluations at the optimal conditions are obtained to be disintegration factor (F_D) of 1.008, which is smaller than all experimental results in the Table 3 and represents a reduction of 5.53% compared to the initial disintegration factor (F_D) of 1.065.

4.5 Confirmation experiments

The confirmation run experiment for the obtained optimum processing parameters was performed in order to verify the adequacy of the quadratic model obtained in this study. The data from the confirmation run and their comparisons with the predicted values for the disintegration factor (F_D) were listed in Table 6. From the analysis of Table 5, the residual and the percentage error calculated are small. The percentage errors between the experimental results and predicted values of F_D lie within −0.45% to 0.48%. All the experimental values for the confirmation run are within the 95% prediction interval. Obviously, the quadratic models obtained for the disintegration factor is excellently accurate.

5 Conclusions

Mathematical model of disintegration factor in the entrance edge of the drilled hole has been carried out to correlate the dominant processing parameters, including the discharge current, pulse time on, duty factor, and capacitance value, in the EDM drilling process of cobalt-bonded tungsten carbide. An experimental plan of a face-centered CCD based on the RSM was employed to carry out the experimental study. The influences of processing parameters on the performance characteristics in the EDM process of cobalt-bonded tungsten carbide were analyzed based on the developed mathematical model to yield the following conclusions:

1. The results of ANOVA and comparisons of experimental data represent that the mathematical model of the value of disintegration factor is fairly well fitted with the experimental values with a 95% confidence interval.
2. The disintegration factor is principally influenced by the interaction effect of discharge current with capacitance value, the capacitance value, and the quadratic term of duty factor with contributions of 14.94%, 13.47%, and 11.96%, respectively.
3. The disintegration factor generally increases with the increase of discharge current and pulse time on. This trend is subjected to the status of input discharging energy which is determined by the discharge current and pulse time on.
4. The disintegration factor increases with the increase of duty factor within the lower value of discharge current. But it decreases within the status of high discharge current.
5. The disintegration factor decreases with an increase of capacitance value within the high value of duty factor and discharging current.
6. Using the SAO method of RSM, the optimal setting of processing parameters are found to be discharge current (I_P) of 4.95A, pulse time on (τ_P) of 16.68 μs, duty factor (D_F) of 0.84, and capacitance value (C_V) of 0.91 μf. For drilling the cobalt-bonded tungsten carbide in the EDM process, the optimal value of disintegration factor presents the reduction of 5.53%, which is compared to the results of the initial processing parameters.

References

1. Schwartz MM (1995) Engineering applications of ceramic materials. Am Soc Metals, Metals Park, Ohio. ISBN:087170207x
2. Klocke F (1997) Modern approaches for the production of ceramic components. J Eur Ceram Soc 17:457–465
3. Allor RL, Jahanmir S (1996) Current problems and future directions for ceramic machining. Am Soc Bull 75(7):40–43
4. Snoeys R, Staelens F, Dekeyser W (1986) Current trends in nonconventional material removal processes. Ann CIRP 35 (2):467–476
5. McGeough JA (1988) Advanced methods of machining. Chapman & Hall, New York, ISBN:0412319705
6. Jeswani ML (1979) Small hole drilling in EDM. Int J Mach Tool Des Res 19:165–169
7. Jain VK (1989) Analysis of electrical discharge drilling of a precision blind hole in HSS using bit type of tool. Microtecnic 2:34–40
8. Uno Y, Okada A, Okamoto Y, Yamazaki K, Risbud SH, Yamada Y (1999) High efficiency fine boring of monocrystalline silicon ingot by electrical discharge machining. Precis Eng 23:126–133
9. Wang CC, Yan BH (2000) Blind-hole drilling of Al2O3/6061 Al composite using rotary electro-discharge machining. J Mater Process Technol 102:90–102
10. Asokan T, Reddy SS, Costa PDE (2000) Electrical discharge drilling of titanium alloys for aerospace applications. Proceedings of 19th AIMTDR conference, IIT Madras, Chennai, pp 161–165
11. Mohan B, Rajadurai A, Satyanarayana KG (2002) Effect of SiC and rotation of electrode on electric discharge machining of Al–SiC composite. J Mater Process Technol 124:297–304
12. Kumagai S, Misawa N, Takeda K, Abdukarimov ET (2004) Plasma-applied machining of a narrow and deep hole in a metal

using a dielectric-encased wire electrode. Thin Solid Films 457:180–185
13. Pham DT, Ivanov A, Bigot S, Popov K, Dimov S (2007) An investigation of tube and rod electrode wear in micro EDM drilling. Int J Adv Manuf Technol 33:103–109
14. Kuppan P, Rajadurai A, Narayanan S (2008) Influence of EDM process parameters in deep hole drilling of Inconel 718. Int J Adv Manuf Technol 38:74–84
15. Myers RH, Montgomery DC (1995) Response surface methodology: process and product optimization using designed experiments. Wiley, New York, ISBN:0470174463
16. Khuri AI, Cornell JA (1996) Response surfaces, designs and analyses. Marcel Dekker, New York, ISBN:0824776534
17. Montgomery DC (2001) Design and analysis of experiments. Wiley, New York, ISBN:0471487357
18. Davim JP, Gaitonde VN, Karnik SR (2008) An investigative study of delamination in drilling of medium density fibreboard (MDF) using response surface models. Int J Adv Manuf Technol 37:49–57
19. Palanikumar K (2008) Application of Taguchi and response surface methodologies for surface roughness in machining glass fiber reinforced plastics by PCD tooling. Int J Adv Manuf Technol 36:19–27
20. Çaydaş U, Hasçalik A (2008) Modeling and analysis of electrode wear and white layer thickness in die-sinking EDM process through response surface methodology. Int J Adv Manuf Technol 38:1148–1156
21. Munda J, Bhattacharyya B (2008) Investigation into electro-chemical micromachining (EMM) through response surface methodology based approach. Int J Adv Manuf Technol 35: 821–832
22. Lin BT, Jean MD, Chou JH (2007) Using response surface methodology with response transformation in optimizing plasma spraying coatings. Int J Adv Manuf Technol 34:307–315